

Feasibility of Two-Dimensional Quantitative Sonoelastographic Imaging

Kenneth Hoyt, Benjamin Castaneda, and Kevin J. Parker

Rochester Center for Biomedical Ultrasound and Department of Electrical and Computer Engineering,
University of Rochester, Rochester, NY 14627 USA

Abstract—In this paper, a two-dimensional (2D) quantitative sonoelastographic technique for estimating local shear wave speeds from slowly propagating shear wave interference patterns (termed crawling waves) is presented. Homogeneous tissue-mimicking phantom results demonstrate the ability of quantitative sonoelastographic imaging to accurately reconstruct the true underlying shear wave speed distribution as verified using mechanical measurements. From heterogeneous phantoms containing a 5 or 10 mm stiff inclusion, results indicate that increasing the estimator kernel size increases the transition zone length about boundaries. Contrast-to-noise ratio (CNR) values from quantitative sonoelastograms obtained in heterogeneous phantoms reveal that the 2D quantitative sonoelastographic imaging technique outperforms the one-dimensional (1D) precursor in terms of image noise minimization and contrast enhancement. Experimental results from an embedded porcine liver specimen with an induced radiofrequency ablation (RFA) lesion validate 2D quantitative sonoelastographic imaging in tissue. Overall, 2D quantitative sonoelastography was shown to be a promising new imaging method to characterizing the shear wave speed distribution in elastic materials.

Keywords—crawling waves; elasticity imaging; shear wave speed estimation; sonoelastography.

I. INTRODUCTION

It is well accepted that pathological changes in biological tissue can alter the underlying elastic properties. In fact, it is this principle that governs lesion detection during palpation-based physical examinations. Since the elastic properties of tissue can span several orders of magnitude, there is optimism in the international research community regarding elasticity-based imaging modalities [1-3] and potential clinical applications.

Sonoelastography is an ultrasound-based elasticity imaging technique that estimates the vibrational response of soft tissue to forced harmonic oscillation [4]. Regarding this particular qualitative method, high and low vibrational amplitudes are surrogates for soft and hard tissue regions, respectively [5]. With the advent of slowly propagating shear wave interference patterns (termed crawling waves) that are generated using two opposing mechanical sources vibrating at slightly offset frequencies [6], the potential for quantitative sonoelastography was established. Owing to the spatial properties of crawling wave patterns, analysis of such provides a local estimate of the underlying tissue elastic properties, namely shear wave speed distributions [7,8].

Recently, a one-dimensional (1D) autocorrelation-based sonoelastographic method was developed for local shear wave speed estimation and imaging [8]. For an opposing source pair and assuming plane wave conditions, crawling waves propagate across the image plane and spatial information is confined to the lateral dimension, which validate use of the 1D quantitative sonoelastographic estimator. However, tissue heterogeneities and shear wavefront distortions can produce deviations from the plane wave assumption. Therefore, a two-dimensional (2D) quantitative sonoelastographic technique incorporating both local axial and lateral data in the estimation process may prove more accurate and robust under these conditions. In this paper, we address this hypothesis by introducing a 2D quantitative sonoelastographic imaging technique and comparing performance to its computationally simpler 1D-based precursor.

II. THEORY

A. One-dimensional quantitative sonoelastography

As shown previously in [8], shear wave interference displacement fields $u(m, n)$ excited using two monochromatic mechanical sources (unity amplitude) can be expressed as

$$u(m, n) = 2 \exp(-\alpha D) \times [\cosh(2\alpha n T_n) + \cos(2k_S n T_n + \Delta k_S n T_n)], \quad (1)$$

where m and n are integer values denoting axial and lateral coordinates, respectively, α denotes the shear wave attenuation coefficient, D is the distance between opposing mechanical sources, T_n denotes the n -axis spatial sampling interval, and k_S and Δk_S denote the shear wave number and difference, respectively. Given the crawling wave displacement field described by (1), the shear wave speed in 1D space can be estimated by evaluating the phase of the 1D autocorrelation function $r(n')$

$$r(n') = \sum_{n=0}^{N-n'-1} \hat{u}^*(n) \hat{u}(n+n'), \quad (2)$$

at lag $n' = 1$, where $\hat{u}(m, n)$ denotes the computed analytic signal of the shear wave displacement data and $*$ denotes complex conjugation. Note that the analytic signal in (2) is computed using Hilbert transform methods or by properly phase shifting consecutive crawling wave frame sequences [8]. For the above discussion, it has been assumed that the 1D data

kernel consists of N lateral samples taken across the image plane (i.e., the axis of crawling wave motion). Finally, the 1D mean shear wave speed estimate $\langle c_s \rangle_{1D}$ for a 1D data kernel is as follows

$$\langle c_s \rangle_{1D} = \frac{2\pi(2f_s + \Delta f_s)T_n}{\tan^{-1}\{\text{Im}[r(1)]/\text{Re}[r(1)]\}}. \quad (3)$$

Since (3) produces a local shear wave speed estimate, 2D spatial distributions are obtained by one-sample shifting the 1D kernel throughout the shear wave displacement field. The resultant matrix is imaged and termed a quantitative sonoelastogram.

B. Two-dimensional quantitative sonoelastography

Similar to the approach described above, the shear wave speed in 2D space can be estimated by evaluating the phase of the 2D autocorrelation function $r(m', n')$ of the analytic signal

$$r(m', n') = \sum_{m=0}^{M-m'-1} \sum_{n=0}^{N-n'-1} \hat{u}^*(m, n) \hat{u}(m+m', n+n'), \quad (4)$$

at lags $(m'=1, n'=0)$ and $(m'=0, n'=1)$. Equation (4) assumes the 2D kernel consists of M axial and N lateral samples. Lastly, the mean shear wave speeds $\langle c_s \rangle_m$ and $\langle c_s \rangle_n$ are estimated relative to the m -axis and n -axis, respectively, by

$$\langle c_s \rangle_m = \left| \frac{2\pi(2f_s + \Delta f_s)T_m}{\tan^{-1}\{\text{Im}[r(1,0)]/\text{Re}[r(1,0)]\}} \right| \quad (5)$$

and

$$\langle c_s \rangle_n = \left| \frac{2\pi(2f_s + \Delta f_s)T_n}{\tan^{-1}\{\text{Im}[r(0,1)]/\text{Re}[r(0,1)]\}} \right|, \quad (6)$$

where T_m denotes m -axis spatial sampling interval along.

Consideration of (5) and (6) allows definition of an angular component

$$\theta = \tan^{-1}\left(\langle c_s \rangle_m / \langle c_s \rangle_n\right), \quad (7)$$

and realization of a 2D mean shear wave speed estimate $\langle c_s \rangle_{2D}$ expressed as

$$\langle c_s \rangle_{2D} = \langle c_s \rangle_n \sin \theta. \quad (8)$$

By noting the following trigonometric relationship

$$\tan^{-1} x = \sin^{-1}\left(x / \sqrt{x^2 + 1}\right) \quad (9)$$

and combining with (7) and (8) results in the following

$$\langle c_s \rangle_{2D} = \frac{\langle c_s \rangle_m}{\sqrt{\left(\langle c_s \rangle_m / \langle c_s \rangle_n\right)^2 + 1}}. \quad (10)$$

In the derivation of (10) we assume plane wave conditions for the region defined by our kernel size and that the elastic medium is approximately homogeneous. Since (10) produces a local shear wave speed estimate, 2D spatial distributions are obtained by one-sample shifting the kernel throughout the shear wave displacement field.

III. MATERIALS AND METHODS

Crawling wave data sets were collected from homogeneous and heterogeneous elasticity phantoms. Quantitative sonoelastograms were generated using the local 1D and 2D shear wave speed estimation techniques described in the Section II. Quantitative sonoelastograms from the homogeneous phantom were analyzed and shear wave speed statistics were computed and compared to mechanical testing measurements performed on phantom samples (i.e., ground truth values) to assess estimator accuracy. Regarding heterogeneous phantom results, which contained a 5 mm or 10 mm stiff spherical inclusion in an otherwise homogeneous background, quantitative sonoelastograms were analyzed for lesion detection and contrast.

To demonstrate the potential for quantitative sonoelastographic imaging in tissue, a fresh porcine liver was obtained after slaughter and stored in saline solution. Subsequently, a localized thermal lesion was created in the liver specimen using radio-frequency ablation (RFA). In general, application of RF energy induced coagulation necrosis and formation of a stiff focal lesion. Lastly, the liver specimen was embedded in a gelatin-based mold to facilitate sonoelastographic imaging.

Two vibration sources (Model 4810, Brüel & Kjaer, Naerum, Denmark) were fitted with surface abraded extensions having an effective contact region of 80 x 10 mm. These extensions were placed in contact with opposing lateral boundaries of the respective scanning materials with the long axis (and induced shear vibration) parallel to, and in line with, the desired image plane (governed by transducer positioning). A two-channel signal generator (Model AFG320, Tektronix, Beaverton, OR, USA) produced two monochrome signals that were passed through power amplifiers (Model 2706, Brüel & Kjaer, Naerum, Denmark) before input to the vibration sources. Phase shifting one of the vibration excitation signals allowed spatial translation of shear wave interference patterns across the image plane and acquisition of one full cycle of wave motion.

For all experiments, a LOGIQ 9 ultrasound scanner (General Electric Medical Systems, Milwaukee, WI USA) modified for sonoelastographic imaging was used with a M12L linear array probe for real-time visualization of crawling wave sonoelastograms. This unit allows access to demodulated data sets (i.e., in-phase and quadrature signals) that were stored and transferred to an external computer for processing quantitative sonoelastograms.

TABLE I. SUMMARY OF QUANTITATIVE SONOELASTOGRAM CONTRAST-TO-NOISE RATIOS (CNR) AS A FUNCTION OF ESTIMATOR KERNEL SIZE (SAMPLES) AND DERIVED FROM 5 MM AND 10 MM INCLUSION PHANTOMS.

Kernel size [M,N]	Contrast-to-noise ratio (CNR)	
	5 mm inclusion phantom	10 mm inclusion phantom
[1,8]	11.3	14.1
[1,12]	11.0	15.4
[1,16]	10.4	14.6
[8,8]	16.7	18.3
[12,12]	26.0	26.8
[16,16]	28.6	31.8

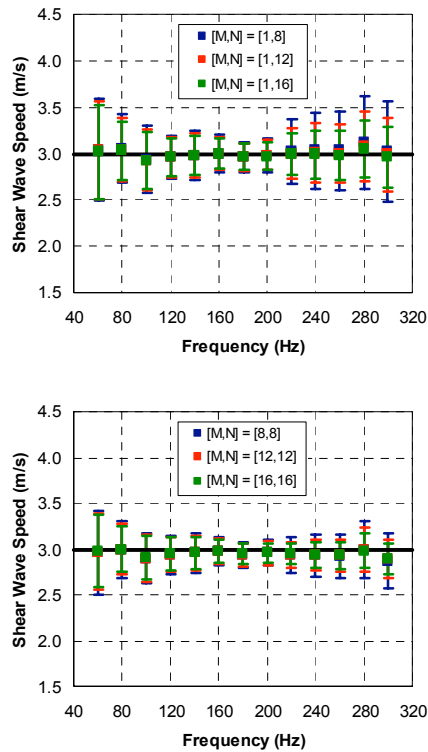


Figure 1. Sonoelastographic shear wave speed estimates from crawling wave image sequences and physical measurements (black). Statistical results are summarized for the 1D (top) and 2D estimation techniques (bottom) and kernel sample sizes indicated.

IV. RESULTS

A summary of homogeneous phantom results are illustrated in Fig. 1. Inspection of these results reveals that using larger kernel sample sizes produces quantitative sonoelastograms with lower noise levels. More specifically, Fig. 1 demonstrates that 2D quantitative sonoelastographic estimates (i.e., shear wave speeds) exhibit less variance than those of the 1D-based technique. Both estimators exhibit higher noise levels at lower frequencies, which is attributed to shear wavelengths being considerably larger than kernel dimensions. However, 2D-based shear wave speed estimates show discernibly lower variances at higher vibration frequencies where attenuation effects are more pronounced and shear wave signal-to-noise levels are lower.

Representative quantitative sonoelastographic results from heterogeneous elasticity phantoms containing either a 5 mm or 10 mm stiff spherical inclusion are presented in Fig. 2. These results illustrate that shear wave interference patterns exhibit localized increases in shear wavelengths corresponding to the inclusion material and characteristic of an elevated shear wave speed. Figure 3 illustrates cross-sectional profiles taken from sets of quantitative sonoelastograms processed using spatial kernels of varying size and using the 1D and 2D shear wave speed estimation techniques. Results indicate that larger kernel sizes produce larger transition zone lengths about the background/inclusion boundary with the overall transition zone length approximately equal to the estimator kernel size.

Therefore, a fundamental tradeoff exists between transition zone length and estimator kernel size. Corresponding quantitative sonoelastogram contrast-to-noise ratio (CNR) values from heterogeneous phantoms are listed in Table 1. Notice that the 2D sonoelastographic estimator outperforms the 1D version for a given kernel size in terms of image noise minimization and contrast enhancement. However, since local shear wave speed values are mean value estimates for a given kernel of shear wave displacement data, utilizing kernel sizes comparable to lesion size implies that a majority of spatial information may be obtained from the softer background material and, thus, lead to an underestimation of the true shear wave speed in the stiffer inclusion.

Experimental sonoelastographic results from an embedded porcine liver specimen with induced RFA lesion are depicted in Fig. 4. Although no discernible lesion is evident in the B-scan image, quantitative sonoelastograms reveal a focal lesion in the image plane characterized by an elevated shear wave speed distribution. Furthermore, inspection of 1D and 2D-based quantitative sonoelastograms reveals less noise artifacts and a more consistent lesion boundary for the latter when compared to the gross pathology photograph albeit with possible misregistration between image planes.

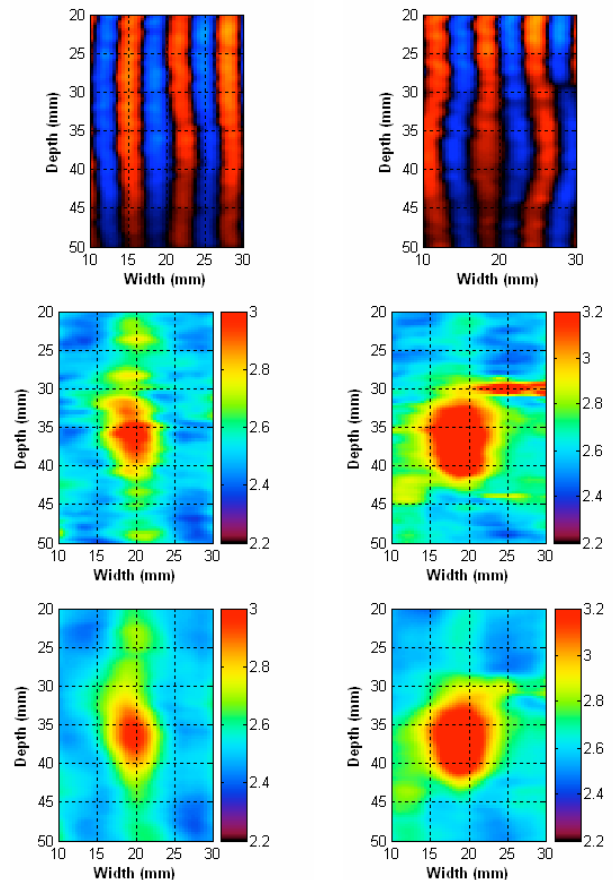


Figure 2. Representative crawling wave (top) and shear wave speed sonoelastograms from phantoms with a 5 mm (left) or 10 mm (right) stiff spherical inclusion and excited using a shear wave vibration frequency of 200 Hz. Quantitative sonoelastograms (units of m/s) were produced using kernel sizes [1,12] and [12,12] corresponding to the 1D and 2D shear wave speed sonoelastographic estimators, middle and bottom, respectively.

V. CONCLUSIONS

A 2D quantitative sonoelastographic estimator was presented and shown to outperform a 1D-based technique in terms of minimizing shear wave speed estimate noise and image artifacts. For both approaches, increasing the estimator kernel size reduces noise levels but inherently lowers spatial resolution. Results from homogeneous elastic phantoms demonstrate the ability of quantitative sonoelastographic imaging to reconstruct the true underlying shear wave speed distributions as verified using mechanical measurements on phantom samples. From heterogeneous elastic phantom results, sonoelastogram CNR values reveal that the 2D quantitative sonoelastographic estimator outperforms the 1D-based approach for a given kernel size in terms of image noise minimization and contrast enhancement. Furthermore, results also indicate that increasing the estimator kernel size increases the transition zone length about boundaries in heterogeneous elastic mediums. Experimental sonoelastographic shear wave speed imaging results from an embedded porcine liver specimen with a RFA induced lesion were presented demonstrating potential for quantitative imaging in tissue. Overall, 2D shear wave speed estimation coupled with crawling wave sonoelastographic imaging was shown to be a promising new quantitative approach to characterizing the mechanical properties of elastic materials.

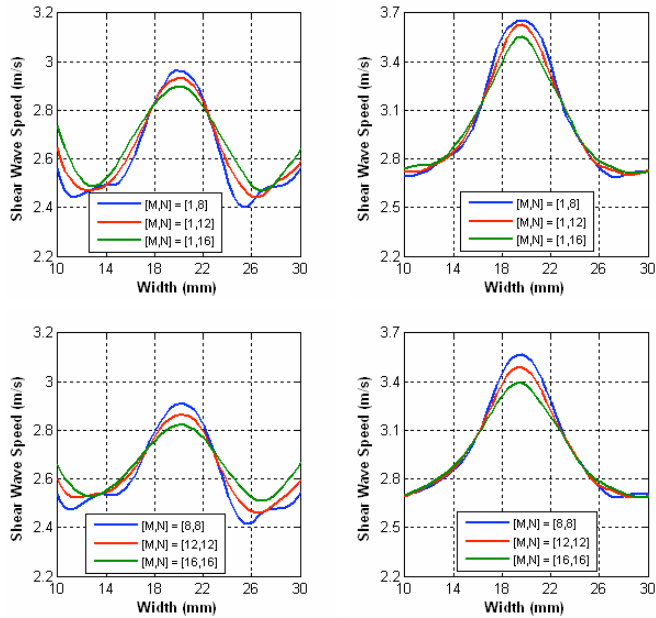


Figure 3. Cross-sectional plot profiles derived from 1D (top) and 2D (bottom) shear wave speed sonoelastographic results. Plots illustrate the transition zone length and image contrast, as a function of estimator kernel size, between the soft background material and stiff inclusions.

ACKNOWLEDGMENT

This research is supported by NIH Grant 5 R01 AG016317-06.

REFERENCES

- [1] L. Gao, K.J. Parker, R.M. Lerner, and S.F. Levinson, "Imaging of the elastic properties of tissue – A review," *Ultrasound Med. Biol.*, vol. 22, pp. 959-977, 1996.
- [2] J. Ophir, S.K. Alam, B. Garra, F. Kallel, E. Konofagou, T. Krouskop, and T. Varghese, "Elastography: Ultrasonic estimation and imaging of the elastic properties of tissues," *Proc. Instn. Mech. Engrs.*, vol. 213, pp. 203-233, 1999.
- [3] J. Greenleaf, M. Fatemi, and M. Insana, "Selected methods for imaging elastic properties of biological tissues," *Annu. Rev. Biomed. Eng.*, vol. 5, pp. 57-78, 2003.
- [4] R.M. Lerner, K.J. Parker, J. Holen, R. Gramiak, and R.C. Waag, "Sonoelasticity: Medical elasticity images derived from ultrasound signals in mechanically vibrated targets," *Acoust. Imaging*, vol. 16, pp. 317-327, 1988.
- [5] K.J. Parker, D. Fu, S.M. Gracewski, F. Yeung, and S.F. Levinson, "Vibration sonoelastography and the detectability of lesions," *Ultrasound Med. Biol.*, vol. 24, pp. 1937-1947, 1998.
- [6] Z. Wu, L.S. Taylor, D.J. Rubens, and K.J. Parker, "Sonoelastographic imaging of interference patterns for estimation of the shear velocity of homogeneous biomaterials," *Phys. Med. Biol.*, vol. 49, pp. 911-922, 2004.
- [7] Z. Wu, K. Hoyt, D.J. Rubens, and K.J. Parker, "Sonoelastographic imaging of interference patterns for estimation of shear velocity distributions in biomaterials," *J. Acoust. Soc. Am.*, vol. 120, pp. 535-545, 2006.
- [8] K. Hoyt, K.J. Parker, and D.J. Rubens, "Real-time shear velocity imaging using sonoelastographic techniques," *Ultrasound Med. Biol.*, vol. 33, pp. 1086-1097.

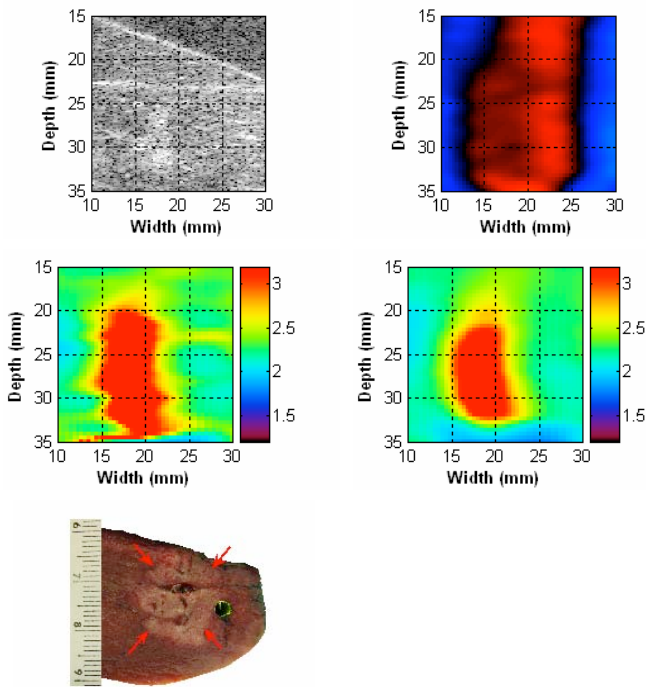


Figure 4. Sonoelastographic results from porcine liver specimen with RFA lesion. Tissue specimen was embedded in gelatin and crawling waves were excited using a vibration frequency of 60 Hz. Results depict the B-scan image (top left), shear wave interference patterns (top right), shear wave speed sonoelastograms (units of m/s) produced using sample kernel sizes of [1,12] (middle left) and [12,12] (middle right) and gross pathology photograph with lesion demarcated by arrows (bottom left).